This document is the accepted manuscript version of the following article:
Gysel, M., Weingartner, E., & Baltensperger, U. (2002). Hygroscopicity of aerosol particles at low temperatures. 2. Theoretical and experimental hygroscopic properties of laboratory generated aerosols. Environmental Science and Technology, 36(1), 63-68.
https://doi.org/10.1021/es010055g

Hygroscopicity of aerosol particles at low temperatures

Part II: Theoretical and experimental hygroscopic properties of laboratory generated aerosols

M. Gysel, E. Weingartner* and U. Baltensperger

Laboratory of Atmospheric Chemistry
Paul Scherrer Institut, 5232 Villigen, Switzerland

* Corresponding author: Ernest Weingartner
Paul Scherrer Institut
Laboratory of Atmospheric Chemistry
CH-5232 Villigen, Switzerland
Email: ernest.weingartner@psi.ch
Phone: 0041 56 310 2405
Fax: 0041 56 310 4525

Abstract

A Hygroscopicity Tandem Differential Mobility Analyzer (H-TDMA) system has been used to measure hygroscopic growth curves and deliquescence relative humidities (DRH) of laboratory generated $(NH_4)_2SO_4$, NaCl, and $NaNO_3$ particles at temperatures T = 20°C and -10°C. Good agreement (better than 3.5%) between measured growth curves and Köhler theory was found using empirical temperature and concentration dependent values for water activity, solution density, and surface tension. The measured growth curves only experience a small temperature dependence in the observed temperature range. Therefore, to a first approximation, it is possible to neglect the temperature dependence of the water activity for theoretical calculations in the temperature range –10°C < T < 25°C. The small differences between experiment and theory, which were predominantly observed for NaCl particles, are probably caused by a small amount of water adsorbed on the “dry” crystals. It was also observed that these particles experience a significant restructuring at relative humidity RH < DRH, which was also taken into account for a comparison with theoretical curves. If salt particles are used for instrument calibration, precautions regarding the dry particle diameter have to be taken.

Revised version submitted to ES&T

Introduction

Atmospheric aerosols contain a large fraction of ionic species (*1*). Most of these species are hygroscopic by nature and exhibit the properties of deliquescence and efflorescence under atmospheric conditions. The hygroscopic properties are important factors affecting air quality, visibility degradation, radiation forcing, and climate change. The relative humidity (RH) dependence of light scattering is one of the parameters needed to estimate the direct climate forcing by aerosol particles (*2,3*). The total scattering cross section of a particle is affected by hygroscopic particle growth particularly in two ways. On the one hand the cross section of the particles increases, and on the other hand the Mie scattering efficiency of particles changes (*4*). Thus, the dry particle size distribution and the hygroscopic growth factors of the particles in humid air must be known to model the humidity dependence of the light scattering of an aerosol. The growth factors of mixed salt solutions can be determined experimentally. Approximations from single salt data are possible, but precise predictions are still an open area of research.

While a number of techniques are available (*5-7*), Hygroscopicity Tandem Differential Mobility Analyzer (H-TDMA) systems are usually used for the determination of the hygroscopic properties of aerosol particles in field experiments. If analysis is to be conducted in the free troposphere where typical temperatures are below 0°C, then measurements should ideally be conducted under ambient conditions, as a change in temperature may significantly alter the particle composition. Therefore, a new H-TDMA system working in the temperature range from -20°C to 30°C was developed (*8*).

While Part I (*8*) describes the system and presents first field measurements at T = -10°C, this paper compares experimental growth factors of different salts with theoretical values. The growth factors of laboratory generated single salt (e.g. NaCl or $(NH_4)_2SO_4$) particles are often used for H-TDMA calibrations. It will be shown that a number of precautions have to be taken into account because the initial dry diameter of these salts may differ from the true volume equivalent diameter by two reasons, i.e. the nonspherical shape and the water content of the dry particles. To avoid this problem, the RH in our setup was determined and calibrated separately by a direct and highly accurate measurement.

In this study, the hygroscopic properties at different temperatures of laboratory generated single salt $(NH_4)_2SO_4$ (ammonium sulfate), NaCl (sodium chloride) and $NaNO_3$ (sodium

nitrate) aerosols were investigated. These salts are common constituents of natural aerosols. Sulfates are a major fraction of the natural ionic aerosol fraction. NaCl is a constituent of maritime aerosols. $NaNO_3$ is formed by the reaction of sea salt with nitric acid from polluted air masses. Growth curves in humid air and the deliquescence relative humidity (DRH) of D_0 = 100 nm particles were measured at 20°C and at -10°C. In addition, the growth factors of D_0 = 50 nm and 100 nm particles at 90% RH with respect to liquid water (at 20°C) or to ice (at -10°C) were measured to verify the influence of the Kelvin effect. In this context the independent RH measurement allows a comparison of experimental data with theoretical values to be conducted.

Experimental

The growth factors of salt particles were measured with the H-TDMA system described in detail in Part I (*8*). Briefly, a narrow size range of a polydisperse dry aerosol was selected with a first Differential Mobility Analyzer (DMA). This monodisperse aerosol was then humidified and the resulting size of the wet particles was measured with a Scanning Mobility Particle Sizer (SMPS) consisting of a second DMA and a Condensation Particle Counter. To improve the growth factor measurement accuracy, the dry particle size exiting the first DMA was periodically checked with the second DMA. The RH was determined by measurement of the system temperature and sheath air dew point using dew point sensors. The measurement uncertainty of the RH depends to a first approximation only on the relative calibration difference between the temperature and the dew point, which is better than 0.2°C.

Artificial aerosol particles were generated by atomization of about 0.02 weight percent salt solutions ($(NH_4)_2SO_4$, purity >99.5%, Fluka; NaCl, >99.5%, Merck; $NaNO_3$, >99%, Merck) in deionized water (18 MΩ·cm, Millipore). The atomizer (TSI 3076 type) was operated with artificial air (80% N_2 >99.999%, 20% O_2 >99.995%). The solution droplets were dried in a custom-built diffusion dryer (residence time ≈ 300 s).

Theory

Köhler Theory

The Köhler theory of the growth of aqueous solution droplets in humid air is described in detail in Pruppacher and Klett (*9*). In the equilibrium state, the RH is equal to the ratio between the vapor pressure over the solution droplet e_d and the saturation vapor pressure of water e_w.

$$RH[\%] = 100\frac{e_d}{e_w} \tag{1}$$

The Köhler equation gives the relation between the droplet diameter D and the equilibrium RH:

$$\frac{e_d}{e_w} = a_w S_{Kelvin} = a_w \exp\left(\frac{4M_w\sigma_{sol}}{RT\rho_w D}\right) \tag{2}$$

Where a_w is the water activity, S_{Kelvin} the Kelvin correction factor, M_w the molar mass and ρ_w the density of water, σ_{sol} the surface tension of the solution, R the ideal gas constant and T the temperature. The vapor pressure over the solution droplet is influenced by the Kelvin and the solution effect. The Kelvin effect describes the increase of the vapor pressure over a curved surface relative to a flat surface. It appears in eq 2 as the factor S_{Kelvin}. Dissolved molecules or ions lead to a decrease of the vapor pressure over the solution relative to pure water. The equilibrium RH over a (flat) solution depends on the solute concentration and species and on the temperature, and it is defined as the water activity a_w. For diluted solutions the water activity can be approximated by the molar ratio of the water (Raoult's law), but this approximation should not be applied for concentrated solutions (RH < 90%).

The growth factor g of a spherical particle is defined as the ratio between the particle diameter D in humid air and the volume equivalent diameter D_0 of the solid particle:

$$g(RH) = \frac{D(RH)}{D_0} \tag{3}$$

Theoretical growth factors can be calculated from the solution concentration c_{sol} (in mass percent), the solution density ρ_{sol} and the salt density ρ_s by:

$$g \equiv \frac{D}{D_0} = \left(\frac{\rho_s}{\frac{c_{sol}}{100}\rho_{sol}} \right)^{1/3} \qquad (4)$$

With the water activity a_w, the surface tension σ_{sol} and the volume equivalent diameter D_0, the equilibrium RH corresponding to this growth factor can be calculated for concentrated solutions (eq 2). The empirical values of solution density, water activity, and surface tension as a function of concentration and temperature used for the theoretical calculations are listed in the Appendix.

Below 0°C the equilibrium vapor pressures over liquid water and ice are different. The Köhler theory (eq 2) is valid for liquid droplets at any temperature. For this reason RH always means the humidity relative to the saturation vapor pressure of liquid water if not otherwise stated.

Hysteresis Effect

The equilibrium size of salt particles in humid air often shows a hysteresis effect depending on their RH history. A solid particle exposed to increasing RH does not significantly change its size until the DRH is reached and a solution droplet is formed. At the DRH the equilibrium droplet size given by the Köhler equation (eq 2) corresponds to a saturated solution droplet. Because of the Kelvin effect, the DRH increases with decreasing particle diameter. A theoretical calculation of the DRH of NaCl particles as a function of the particle size (*10*) shows that the influence of the Kelvin effect on the DRH can be neglected for particles larger than D_0 = 100 nm. A further increase of the RH leads to droplet growth in accordance with Köhler theory. Once in the liquid phase, the particle can exist in a metastable equilibrium state as a supersaturated solution droplet at a RH below the DRH. The efflorescence relative humidity (ERH) is given by the supersaturation at which crystallization takes place. Due to insoluble impurities, the crystallization can occur above the ERH.

Results

Shape Correction and Restructuring below DRH

Theoretical growth factors are calculated with the volume equivalent diameter D_0, while the H-TDMA measures the mobility diameter D_{mob}, which is only equal to the volume equivalent diameter D_0 for spherical particles. It is well known (*9*) that dry $(NH_4)_2SO_4$ particles are virtually spherical, while dry NaCl particles are cubic. Therefore the measured mobility diameter D_{mob} of the dry NaCl particles must be shape corrected to get the volume equivalent diameter D_0. Because the solution droplets are always spherical, no shape correction is applied for droplets. The aerodynamic drag forces F_{drag} on non-spherical particles are described with a modified Stokes' law (*11*):

$$F_{drag} = \frac{3\pi\eta v D_0 \chi}{C_c(D_0)} \tag{5}$$

where η is the gas viscosity, v the velocity, χ the dynamic shape factor and D_0 the volume equivalent diameter of the particle. For spherical particles, χ_{sphere} has per definition the value 1, while for cubic particles, χ_{cube} is equal to 1.08 (*12*). The Cunningham slip correction factor C_c is given in Hinds (*12*):

$$C_c = 1 + \frac{1}{PD}\left[15.60 + 7.00\exp\left(-0.059PD\right)\right] \tag{6}$$

where P is the pressure in kPa and D the particle diameter in μm. The relation between the mobility diameter D_{mob} and the volume equivalent diameter D_0 of a cubic particle is:

$$f_{cube} = \frac{D_0}{D_{mob}} = \frac{1}{\chi_{cube}} \frac{C_c(D_0)}{C_c(D_{mob})} \tag{7}$$

For D_0 = 100 nm particles (at 980 mbar air pressure) eq 7 yields a correction factor of f_{cube} = 0.96, which is applied to the experimental mobility diameter D_{mob} of the solid NaCl particles to obtain the volume equivalent diameter D_0.

Figure 1 shows the behavior of solid 100 nm NaCl particles below the DRH at T = 20°C. The particle size decreases by up to 9% when the particles are brought from dry air (RH < 20%) to a RH just below the DRH of ~75%. One can imagine that the reduction of

the electrical mobility diameter is caused by elimination of particle shape irregularities. The variations between different runs are most probably caused by small variations of the particle generation, such as solution concentration and diffusion dryer condition. Krieger and Braun (*13*) studied deliquescence-efflorescence-cycles of NaCl particles in an electrodynamic trap. Repetitions of this cycle with the same particle showed that the optical properties of the newly formed solid particle changed with each repetition even under very similar conditions. This was attributed to variations in the morphology of the newly crystallized particle. The two points highlighted by the arrows had been exposed to RH above 50% in the humidifier before their size was measured at 20-30% RH. Thus they already experienced a certain restructuring resulting in a smaller size than found for other particles of the same run. This indicates that the restructuring process is to some extent irreversible.

A restructuring was observed for $(NH_4)_2SO_4$ particles as well, but the size reduction was always smaller than 2%. A comparison of all measurements of $(NH_4)_2SO_4$ particles indicates that the restructuring effect is less distinct for smaller particles and for lower temperatures.

In the following, the minimum solid particle diameter D_{min} is chosen to calculate the dry particle volume equivalent diameter D_0, which is used as reference for the experimentally determined growths factors. This choice is justified by the fact that experimental growth factors relative to D_{min} were always reproducible in contrast to growth factors relative to the particle diameter at RH < 20%.

Humidograms

Growth curves of laboratory generated D_0 = 100 nm $(NH_4)_2SO_4$, NaCl, and $NaNO_3$ particles in humid air were measured at 20°C and -10°C. Two to five measurement runs were made per salt and per temperature. The results are presented in Figures 2 to 4. RH always denotes the humidity relative to liquid water. The measurement accuracy at 90% (20°C) and at 81.7% RH (-10°C) is indicated by the error bar in the charts. The experimental growth factors are sorted by "Decreasing RH" and "Increasing RH". Increasing RH means that the particles have not been exposed to higher RH before, which allows the DRH to be measured. Decreasing RH means that the particles have been previously exposed to higher RH. Therefore, if these particles have (not) passed the DRH,

these data points are solution droplets (solid particles) on the upper (lower) branch of the hysteresis curve. For further details, the reader is referred to Part I (*8*). Both $(NH_4)_2SO_4$ and NaCl particles show the hysteresis effect in the growth curve. Starting at low RH, the dry salt particles do not change their size substantially (except for the restructuring described above) until they reach the DRH and a solution droplet is formed. The small particle growth just below the DRH is most probably caused by water adsorption on imperfection sites of the lattice and is discussed in Part I (*8*).

A further increase of the RH leads to particle growth by condensation of water in accordance with Köhler theory. At decreasing RH, the droplets reduce their size by evaporation of water and can exist below the DRH as metastable supersaturated solutions. A further decrease of the RH down to the ERH leads to crystallization of the droplets. In the operational mode used for this experiment, the ERH was not measured. An upper limit for the ERH is given by the lowest data point on the upper branch of the hysteresis, but the difference to the real ERH depends arbitrarily on the measurement cycle. In addition to the experimental values, theoretical growth curves are plotted in Figures 2 to 4. The curves "Theory" are calculated according to eq 2 using salt specific surface tension, solution density, and water activity values. The concentration and temperature dependence of these parameters is considered except for $NaNO_3$ where only water activity values for 25°C were available (see Appendix). In general, the agreement between experiment and theory is very good. A detailed discussion for each salt is given below.

At temperatures below 0°C the formation of ice particles has to be taken into account. Possible processes are the nucleation of ice on solid particles and the freezing of solution droplets. The first process cannot take place in the H-TDMA because the setup is designed such that air is never supersaturated relative to the saturation vapor pressure over ice. The second process depends on the freezing point depression due to the solute. The higher the RH, the more dilute the solution droplets and the lower the freezing point depression. For each temperature, there is a lower limit for the relative humidity, RH* where droplet freezing is theoretically possible. RH* was calculated from empirical freezing point depressions (*14*) and theoretical growth factors (cf. section Theory). It is found that RH* is almost independent of temperature and salt species and has a value slightly higher (≈0.8%) than 100% humidity relative to the ice phase. Therefore, freezing of solution

droplets in the H-TDMA is not expected. This is in accordance with the experimental results, because the measured growth factors agree well with the liquid phase theory (Figures 2b, 3b and 4b).

$(NH_4)_2SO_4$

The experimental results for D_0 = 100 nm $(NH_4)_2SO_4$ particles at 20°C are shown in Figure 2a. The experimental growth factors agree well with the theoretical growth curve. The particles show the hysteresis effect as described above. The deliquescence transition was observed at 80±1.2% RH in good agreement with literature data of 79.9% (*7*) and 80.3% (*15*), respectively.

The experimental results for D_0 = 100 nm $(NH_4)_2SO_4$ particles at -10°C are shown in Figure 2b. The experimental growth factors are 2% smaller than the theoretical values over the whole RH range. This is a relatively large difference compared to the experimental variations between the individual experimental runs. The deliquescence transition was observed at 82.5±1.5% RH in agreement with literature data of 82.0% (*7*) and 82.6% (*15*), indicating that the difference between experiment and theory is real. The constancy of the difference over the whole RH range suggests that the measured minimum diameter at T = -10°C is 2% larger than the real volume equivalent diameter of the particle. This could be caused by remaining small particle shape irregularities at these low temperatures (see above).

The experimental growth factors of the investigated salt particles showed only weak temperature dependence. A theoretical sensitivity analysis was performed and it was found that the Kelvin effect causes a growth factor reduction of 0.2 to 0.3% at -10°C compared to 20°C, and that neglecting the temperature dependence of the water activity causes growth factor errors smaller than 2% at any RH. Therefore, it is a good approximation to use water activity values of 25°C for the temperature range -10°C < T < 25°C. This approximation has the advantage that the concentration dependence of the water activity can be described with a simple 3rd- or 4th-order polynomial compared to the quite extensive semi-empirical water activity models.

NaCl

Solid NaCl particles are cubic, as already mentioned. Therefore, the measured mobility diameters of solid NaCl particles are multiplied by the correction factor f_{cube} = 0.96 to obtain the volume equivalent diameter (see above). The experimental results for D_0 = 100 nm NaCl particles at 20°C are shown in Figure 3a. The NaCl particles show deliquescence at DRH = 75±1.2% at 20°C in agreement with literature data of 75.4% (*15*). The experimental growth factors are 3.5% smaller than the theoretical values over the whole RH range (cf. curve "Theory"). The same difference between experimental and theoretical growth factors of D_0 = 96 nm NaCl particles at 20°C was observed by Krämer et al. (*16*) with a H-TDMA system. The curve "Theory fitted" was fitted to the experimental data by multiplication of the theoretical curve "Theory" with the constant factor 0.965. The excellent agreement of the curve "Theory fitted" with the experimental growth factors supports the assumption that the measured minimum diameter (including the cube correction) is still 3.5% larger than the volume equivalent diameter corresponding to the real amount of salt. Weis and Ewing (*17*) measured the water content of 200 nm NaCl particles with infrared absorption spectroscopy. They observed that at RH = 25% NaCl particles contain water in pores and adsorbed on the surface, resulting in a H_2O : NaCl molar ratio of about 0.08. The 3.5% difference between experiment and theory observed in this study corresponds to a molar ratio of about 0.17. This is reasonable because in this study the particles are smaller and the minimum diameter was measured at about 70% RH.

The experimental results for D_0 = 100 nm NaCl at -10°C particles are shown in Figure 3b. The deliquescence transition takes place at 75±1.5% and is in agreement with literature data of 76.1% (*15*) within the measurement accuracy. Similar to the results at 20°C the experimental growth factors at -10°C are 3.5% smaller than the theoretical values over the whole RH range (cf. curve "Theory").

Again, the amount of water adsorbed on the particles at RH < DRH reduces the hygroscopic growth factors and might even depend on the particle generation conditions. Therefore, care has to be taken when the hygroscopic growth of salt particles is used for the calibration of H-TDMA measurements, even when the minimum diameter just below the DRH is considered.

$NaNO_3$

Figure 4 shows that the $NaNO_3$ particles did not exhibit the deliquescence phenomenon in this experiment. The continuous growth of the particles indicates that they were present as solution droplets all the time. Literature data (*5*) report a hysteresis effect of $NaNO_3$ particles at 25°C with, a DRH of 74.5% and an ERH between 30% and 0.05%. These measurements were made with the single-particle levitation technique, where lower RH values can be reached than with the diffusion dryer. The minimum RH in this experiment (about 6% after the diffusion dryer) was obviously not low enough for the spontaneous crystallization of the $NaNO_3$ particles. Because of the missing crystallization, the $NaNO_3$ particles are in the liquid phase already in the first DMA and have a diameter larger than the volume equivalent diameter of the solute $NaNO_3$. Thus, the droplet diameter measured at the minimal RH (RH_{min}) is divided by the theoretical growth factor $g(RH_{min})$ (1.02 at 20°C and 6% RH and 1.05 at -10°C and 15% RH, respectively) to deduce the volume equivalent diameter D_0.

The results for D_0 = 100 nm $NaNO_3$ particles at 20°C and at -10°C are shown in Figure 4. The theoretical growth factors (cf. curves "Theory") are calculated with empirical water activity values at 25°C. Again, neglecting the temperature dependence of the water activity yields a good approximation (see above). As the $NaNO_3$ particles do not show the hysteresis effect, there is no difference between the growth factors measured at increasing and decreasing RH. At both temperatures, the experimental results agree with the theory within the measurement accuracy.

Growth Factors

In addition to the growth curves of D_0 = 100 nm particles, some growth curves of D_0 = 50 nm particles were also measured but are not shown here, because the 50-nm particles showed qualitatively the same behavior as the 100-nm particles. Table 1 gives growth factors for the D_0 = 50 nm and 100 nm particles for 90% RH (T = 20°C) and for 81.7% RH (T = -10°C), respectively. The latter RH value is chosen, because 81.7% RH at -10° is equivalent to 90% humidity relative to ice. The cubic shape of NaCl particles and the growth factor of the $NaNO_3$ particles in the first DMA (cf. Results for $NaNO_3$) are taken into account in the experimental values. The experimental growth factors g_{exp} measured in the

RH range 90 ± 3% (T = 20°C) and 81.7 ± 3% (T = -10°C), respectively, were corrected to the desired relative humidity RH_{des} with theoretical growth factor values g_{th}:

$$g_{\exp}(RH_{des}) = g_{\exp}(RH_{\exp})\frac{g_{th}(RH_{des})}{g_{th}(RH_{\exp})} \quad (8)$$

In Table 1, Δg_{exp} is the absolute measurement uncertainty, while g_{th} is the theoretical growth factor. The experimental growth factors agree well with the theoretical values. As discussed above, the differences between theory and experiment for $(NH_4)_2SO_4$ and NaCl particles are probably caused by the water content of the dry particles. Due to the Kelvin effect, the growth factors of the 50-nm particles are smaller than those of the 100-nm particles.

Acknowledgement

This work has been carried out with financial support from the Bundesamt für Bildung und Wissenschaft, BBW (PARTEMIS project). We thank Ulrich Pöschl and Lutz Krämer for helpful discussions and Peter Häberli for his help in experimental work.

Literature Cited

(1) Heintzenberg, J. *Tellus* **1989**, *41B*, 149-160.

(2) Schwartz, S. E. *J. Aerosol Sci.* **1996**, *27*, 359-382.

(3) Charlson, R. J.; Schwartz, S. E.; Hales, J. M.; Cess, R. D.; Coakley, J. A., Jr.; Hansen, J. E.; Hofmann, D. J. *Science* **1992**, *255*, 423-430.

(4) Hegg, D. *J. Geophys. Res.* **1993**, *98*, 18435-18439.

(5) Tang, I. N.; Munkelwitz, H. R. *J. Geophys. Res.* **1994**, *99*, 18801-18808.

(6) McMurry, P. H.; Stolzenburg, M. R. *Atmos. Env.* **1989**, *23*, 497-507.

(7) Onasch, T. B.; Siefert, R. L.; Brooks, S. D.; Prenni, A. J.; Murray, B.; Wilson, M. A.; Tolbert, M. A. *J. Geophys. Res.* **1999**, *104*, 21317-21326.

(8) Weingartner, E.; Gysel, M.; Baltensperger, U. *Environ. Sci. Technol.* **2001**, *submitted*.

(9) Pruppacher, H. R.; Klett, J. D. *Microphysics of Clouds and Precipitation*; 2nd ed.; Kluwer Academic Publishers: Dordrecht, 1997.

(10) Cinkotai, F. F. *Aerosol Science* **1971**, *2*, 325-329.

(11) Willeke, K.; Baron, P. A. *Aerosol Measurement: Principles Techniques and Applications*; Van Nostrand Reinhold: New York, 1993.

(12) Hinds, W. C. *Aerosol Technology: Properties, Behavior, and Measurement of Airborne Particles*; 2nd ed.; John Wiley & Sons, Inc.: New York, 1999.

(13) Krieger, U. K.; Braun, C. *J. Quant. Spect. Rad. Trans.* **2001**, *70*, 545-554.

(14) Lide, D. R. *CRC Handbook of Chemistry and Physics*; 79 ed.; CRC Press: Boca Raton, 1998.

(15) Tang, I. N.; Munkelwitz, H. R. *Atmos. Env.* **1993**, *27A*, 467-473.

(16) Krämer, L.; Pöschl, U.; Niessner, R. *J. Aerosol Sci.* **2000**, *31*, 673-685.

(17) Weis, D. D.; Ewing, G. E. *J. Geophys. Res.* **1999**, *104*, 21275-21285.

(18) Tang, I. N. *J. Geophys. Res.* **1997**, *102*, 1883-1893.

(19) Seinfeld, J. H.; Pandis, S. N. *Atmospheric Chemistry and Physics: From Air Pollution to Climate Change*; John Wiley&Sons, Inc.: New York, 1998.

(20) Chen, J.-P. *J. Atmos. Sci.* **1994**, *51*, 3505-3516.

(21) Pitzer, K. S. *Activity Coefficients in Electrolyte Solutions*; 2nd ed.; CRC Press: Boca Raton, 1991.

(22) Clegg, S. L.; Ho, S. S.; Chan, C. K.; Brimblecombe, P. *J. Chem. Eng. Data* **1995**, *40*, 1079-1090.

(23) Clegg, S. L.; Brimblecombe, P. *J. Chem. Eng. Data* **1995**, *40*, 43-64.

(24) Mokbel, I.; Ye, S.; Jose, J.; Xans, P. *J. Chim. Phys.* **1997**, *94*, 122-137.

Appendix

The Köhler theory (cf. section Theory) gives the relation between the RH and the equilibrium droplet diameter (eq 2). For the calculation of the theoretical growth curves, concentration and temperature dependent (semi-) empirical values of the solution density, surface tension and water activity are needed. All functions and values needed for the calculation are listed in this section.

Solution Density

Densities of salt solutions ρ_{sol} up to high supersaturation are reported in Tang (*18*):

$$\rho_{sol}(T,x) = \rho_w(T) + \sum_i A_i x^i \qquad \text{(A.1)}$$

Where x is the salt concentration in mass percent and T is the temperature. The density ρ_w of pure water is tabulated in Lide (*14*) and the coefficients A_i are listed in Table A1 (*18*).

Solution Surface Tension

The surface tension of pure water σ_w [J/m^2] as a function of temperature T [°C] is given in Seinfeld and Pandis (*19*):

$$\sigma_w(T) = 0.0761 - 1.55 \cdot 10^{-4} \cdot T \qquad \text{(A.2)}$$

The surface tension of a solution σ_{sol} shows in good approximation a linear dependence on the salt molality m_{salt} (*19*):

$$\sigma_{sol}(m_{salt}, T) = \sigma_w(T) + \beta_s m_{salt} \qquad \text{(A.3)}$$

where β_s is a salt specific coefficient and values are listed in Table A2 (*20*).

Water Activity of $(NH_4)_2SO_4$ Solution

The concentration and temperature dependence of the water activity a_w of electrolyte solutions can be described by Pitzer's mole fraction based model (*21*). Model parameters

for $(NH_4)_2SO_4$ are published in Clegg et al. (*22*), and the water activity is calculated by the following equation:

$$\ln(a_w) = \ln(x_w) + \frac{2A_x I_x^{3/2}}{1+\rho I_x^{1/2}} - x_M x_X B_{MX} \exp\left(-\alpha_{MX} I_x^{1/2}\right) - x_M x_X B^1_{MX} \exp\left(-\alpha^1_{MX} I_x^{1/2}\right) + \tag{A.4}$$

$$x_I^2 (W_{w,MX} + (x_I - x_w) U_{w,MX}) + 4 x_w x_M x_X (2 - 3x_w) V_{w,MX}$$

The subscripts *w*, *M*, *X* and *I* stand for the solvent water, the cation NH_4^+, the anion SO_4^{2-} and the sum of these ions, respectively, and *x* is the molar ratio. The model constants ρ, α_{MX} and α^1_{MX} are temperature independent. The Debye-Hückel parameter A_x is given for several temperatures in Clegg and Brimblecombe (*23*). The coefficients B_{MX}, B^1_{MX}, $W_{w,MX}$, $U_{w,MX}$ and $V_{w,MX}$ and their derivatives with respect to temperature are given for 25°C, and they were integrated to other temperatures. All coefficients for the temperatures 20°C and -10°C are listed in Table A3.

Water Activity of NaCl Solution

The water activity a_w is related to the osmotic coefficient ϕ by the following equation:

$$\ln(a_w) = \phi \ln(x_w) \tag{A.5}$$

where x_w is the molar ratio of water.

The concentration and temperature dependence of the osmotic coefficient ϕ of electrolyte solutions can be described by Pitzer's molality based model (*21*):

$$\phi = 1 + \left|z_M z_X\right| f^\phi + m \frac{2\upsilon_M \upsilon_X}{\upsilon} B^\phi_{MX} + m^2 \frac{2(\upsilon_M \upsilon_X)^{3/2}}{\upsilon} C^\phi_{MX} \tag{A.6}$$

where

$$\upsilon = \upsilon_M + \upsilon_X \tag{A.7}$$

$$f^\phi = -\frac{A_\phi I_m^{1/2}}{1 + b I_m^{1/2}} \tag{A.8}$$

$$A_\phi = \frac{1}{3}\left(\frac{2\pi N_0 \rho_w}{1000}\right)^{1/2}\left(\frac{e^2}{DkT}\right)^{3/2} \quad \text{(A.9)}$$

$$B^\phi_{MX} = \beta^{(0)}_{MX} + \beta^{(1)}_{MX} e^{-\alpha I_m{}^{1/2}} \quad \text{(A.10)}$$

$$\beta^{(0)}_{MX}(T) = w_6 + \frac{w_7}{T} + w_8 \ln(T) + w_9 T + w_{10} T^2 + \frac{w_{11}}{T-227} + \frac{w_{12}}{680-T} \quad \text{(A.11)}$$

$$\beta^{(1)}_{MX}(T) = w_{13} + \frac{w_{14}}{T} + w_{15} T + \frac{w_{16}}{T-227} \quad \text{(A.12)}$$

$$C^\phi_{MX} = w_{17} + \frac{w_{18}}{T} + w_{19} \ln T + w_{20} T + \frac{w_{21}}{T-227} \quad \text{(A.13)}$$

The model parameters for NaCl salt are published in Mokbel et al. (*24*). The constants are: molality m of the solution, charge z_M and z_X and stoichiometric factors ν_M and ν_X of the ions M and X, Avogadro's number N_0, Boltzman constant k, density ρ_w and dielectric constant D of water, temperature T [K] and elementary charge e. The model constants b and α have the values 1.2 $kg^{1/2}mol^{-1/2}$ and 2.0 $kg^{1/2}mol^{-1/2}$, respectively. Values for the Debye-Hückel parameter A_ϕ are listed in Pitzer (*21*). The coefficients w_6 to w_{21} for the temperature dependent ion-interaction parameters $\beta^{(0)}_{MX}$, $\beta^{(1)}_{MX}$ and C^ϕ_{MX} are listed in Table A4. The molal ionic strength I_m is defined as $I_m = 0.5\sum_i m_i z_i^2$, where the summation goes over all ions with molalities m_i and charges z_i.

Water Activity of $NaNO_3$ Solution

To our knowledge, there is no literature data available for the calculation of the water activity a_w of $NaNO_3$ solution at temperatures below 0°C. As discussed above (cf. Results) it is a good approximation to neglect the temperature dependence of the water activity at temperatures below 25°C. Therefore, water activity values of $NaNO_3$ solution at the temperature 25°C (*5*) are used for the calculation of the theoretical growth curves at 20°C as well as at -10°C:

$$a_w = 1.0 - 5.52\cdot 10^{-3} x - 1.286\cdot 10^{-4} x^2 - 3.496\cdot 10^{-6} x^3 + 1.843\cdot 10^{-8} x^4 \quad \text{(A.14)}$$

where x is the solute mass percentage.

Figure Captions

Figure 1. Restructuring of 100 nm NaCl particles at 20°C below the deliquescence point. Arrows denote particles that were exposed to RH above 50% before their size was measured at 20-30% RH. Different symbols are given for different runs.

Figure 2. Growth factors of D_0 = 100 nm $(NH_4)_2SO_4$ particles as a function of RH, for T = 20°C (a) and T = -10°C (b).

Figure 3. Growth factors of D_0 = 100 nm NaCl particles as a function of RH, for T = 20°C (a) and T = -10°C (b).

Figure 4. Growth factors of D_0 = 100 nm $NaNO_3$ particles as a function of RH, for T = 20°C (a) and T = -10°C (b).

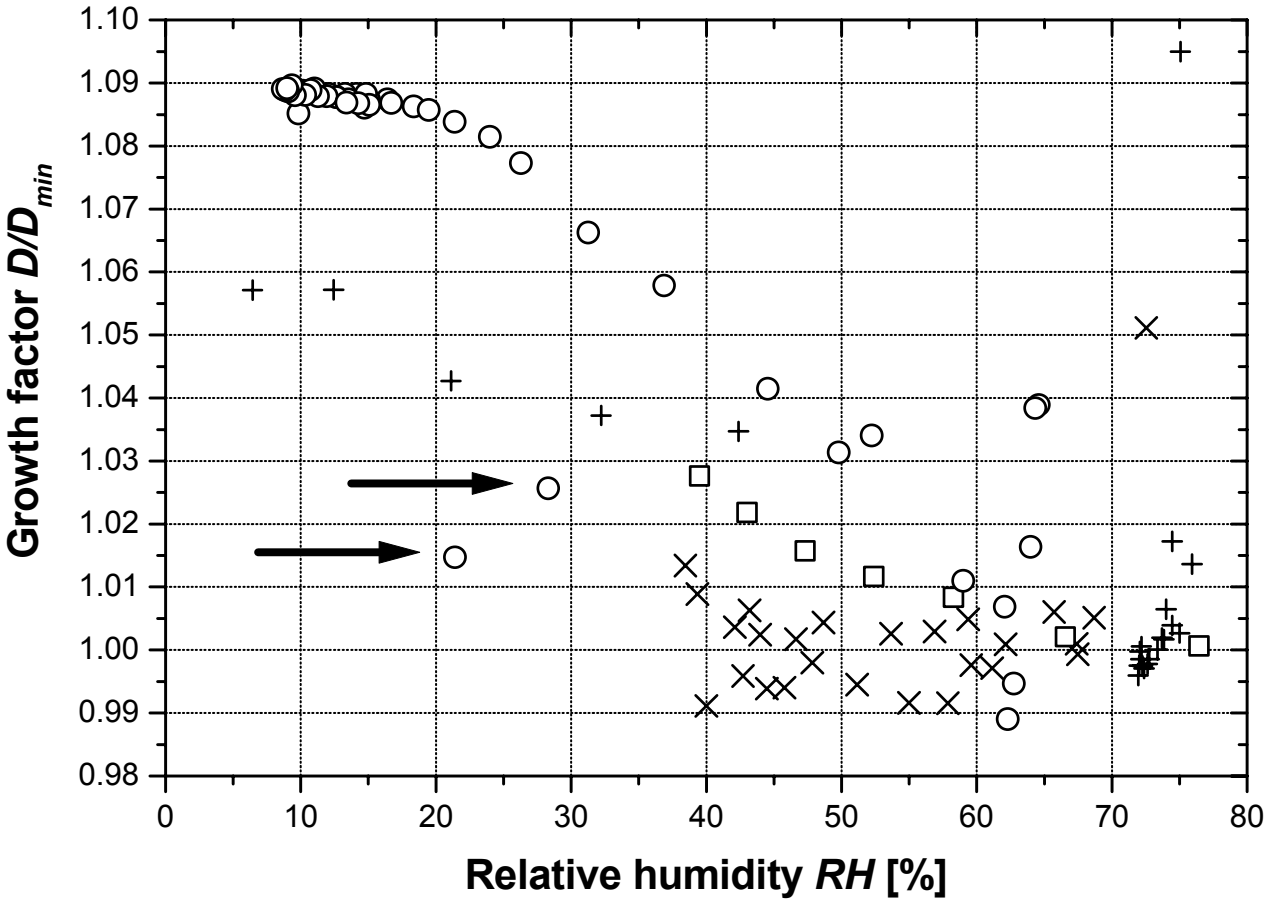
Growth factor D/D_{min}
1.10
1.09
1.08
1.07
1.06
1.05
1.04
1.03
1.02
1.01
1.00
0.99
0.98
0
10
20
30
40
50
60
70
80
Relative humidity *RH* [%]

Figure 1

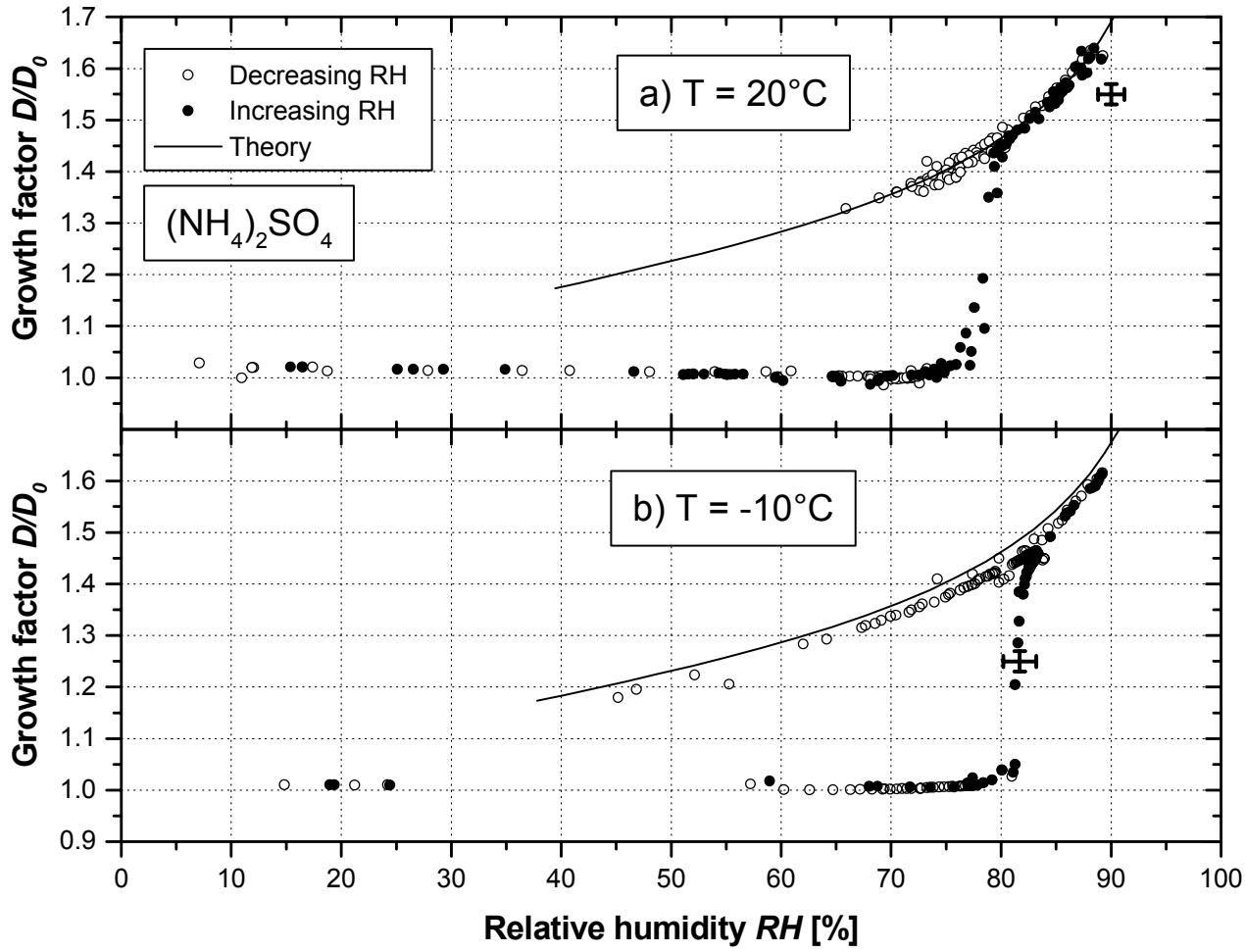
Decreasing RH
Increasing RH
Theory
(NH4)2SO4
a) T = 20°C
b) T = -10°C
Growth factor D/D0
Growth factor D/D0
Relative humidity RH [%]

Figure 2

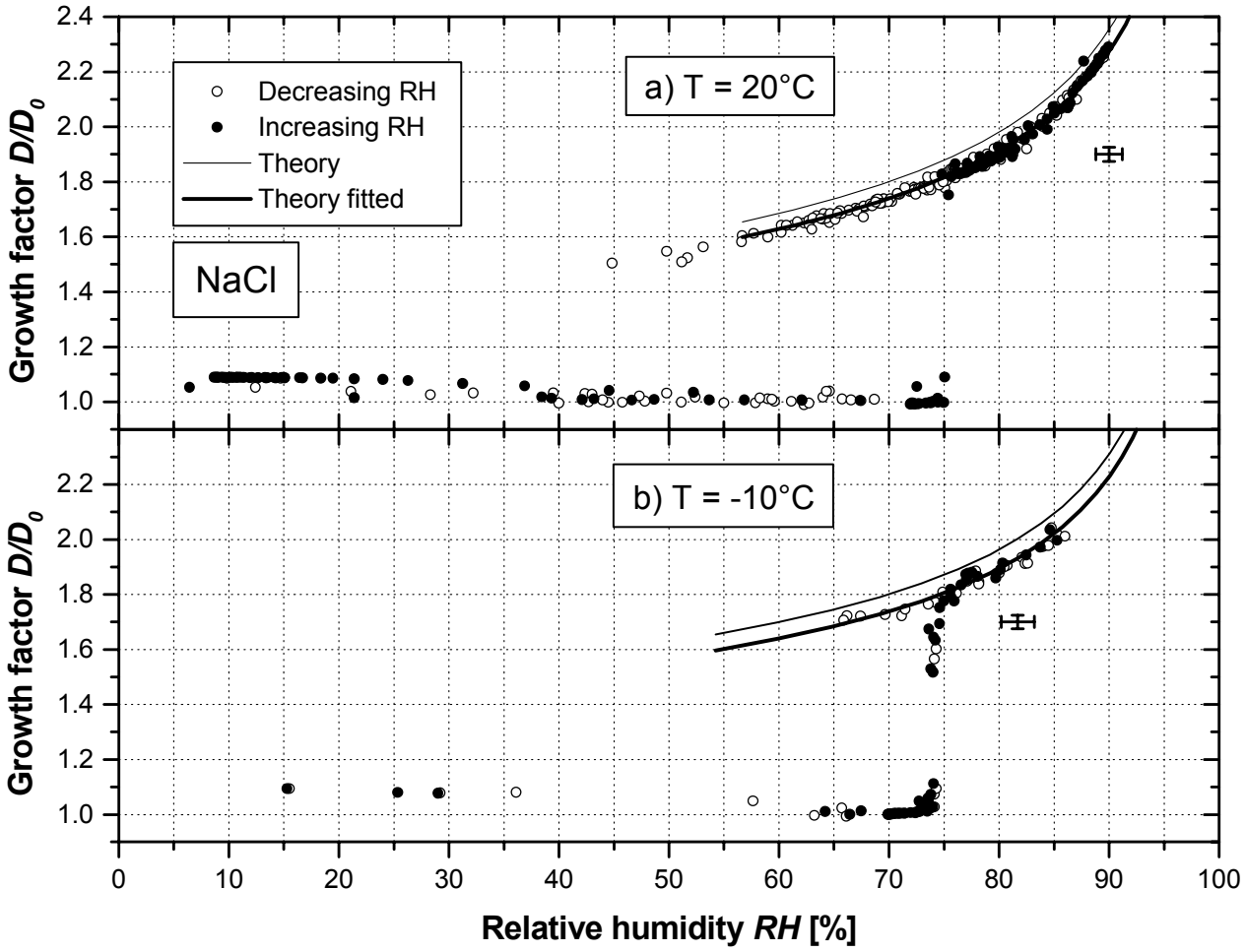
Decreasing RH
Increasing RH
Theory
Theory fitted
NaCl
a) T = 20°C
b) T = -10°C
Growth factor D/D0
Growth factor D/D0
Relative humidity RH [%]

Figure 3

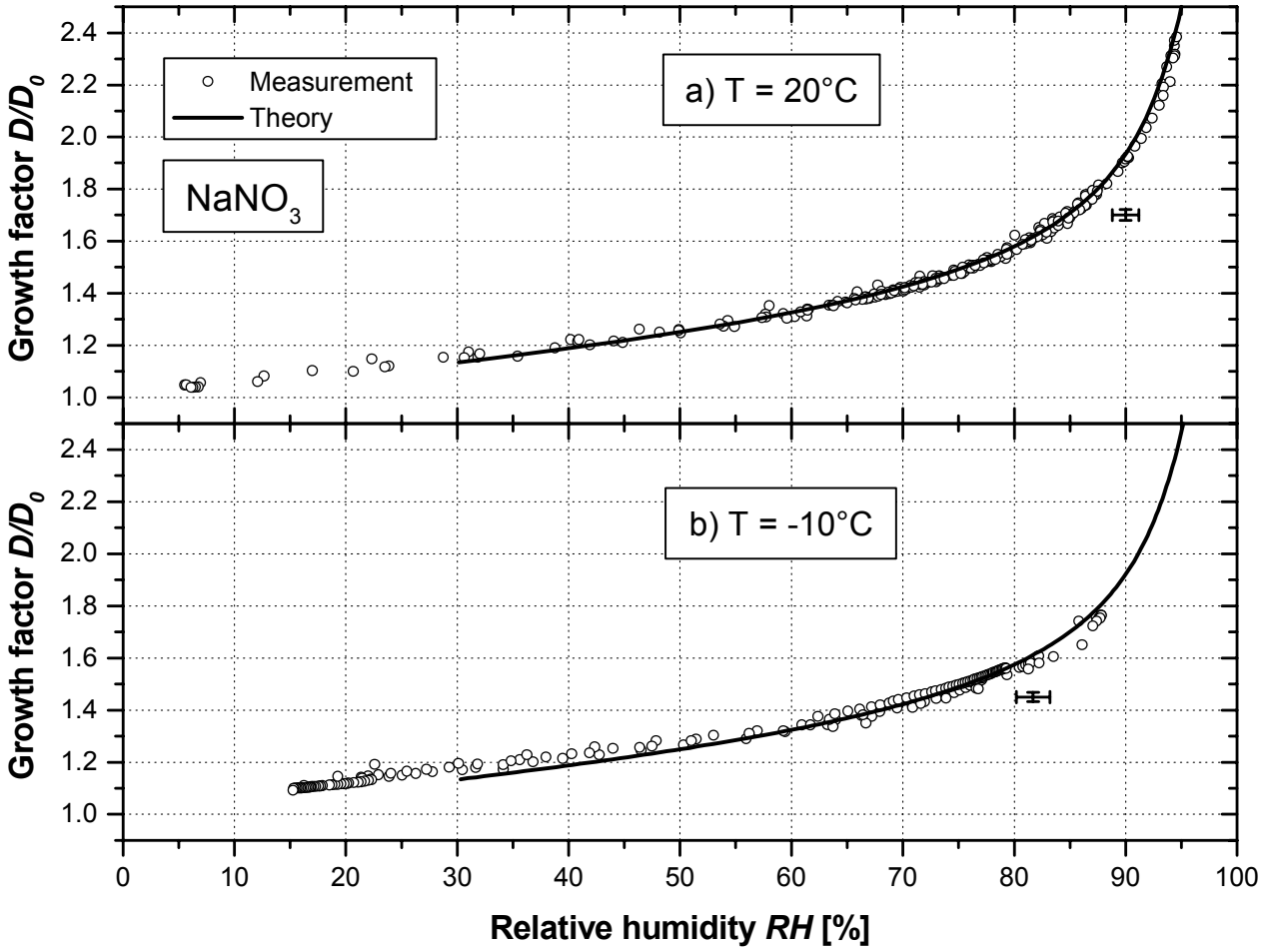
Measurement
Theory
NaNO3
a) T = 20°C
b) T = -10°C
Growth factor D/D0
Growth factor D/D0
Relative humidity RH [%]
1.0
1.2
1.4
1.6
1.8
2.0
2.2
2.4
0
10
20
30
40
50
60
70
80
90
100

Figure 4

Table 1. Growth factors of salt particles, where g_{exp} is the experimental growth factor, Δg_{exp} the absolute measurement uncertainty and g_{th} the theoretical growth factor. At -10°C RH = 81.7% corresponds to 90% humidity relative to ice.

Salt	*T* [°C]	*RH* [%]	D_0 [nm]	$\boldsymbol{g_{exp}}$*	Δg_{exp}	$\boldsymbol{g_{th}}$	$\frac{g_{exp} - g_{th}}{g_{th}}$
$(NH_4)_2SO_4$	20	90	100	**1.68**	0.05	**1.69**	-0.01
$(NH_4)_2SO_4$	20	90	50	**1.66**	0.05	**1.65**	0.01
$(NH_4)_2SO_4$	-10	81.7	100	**1.46**	0.03	**1.49**	-0.02
$(NH_4)_2SO_4$	-10	81.7	50	**1.42**	0.03	**1.46**	-0.03
NaCl	20	90	100	**2.29**	0.08	**2.35**	-0.03
NaCl	20	90	50	**-**	-	**2.30**	-
NaCl	-10	81.7	100	**1.92**	0.04	**2.00**	-0.04
NaCl	-10	81.7	50	**-**	-	**1.97**	-
$NaNO_3$	20	90	100	**1.91**	0.08	**1.94**	-0.01
$NaNO_3$	20	90	50	**1.86**	0.08	**1.88**	-0.01
$NaNO_3$	-10	81.7	100	**1.60**	0.04	**1.61**	-0.01
$NaNO_3$	-10	81.7	50	**1.55**	0.04	**1.59**	-0.02

*The cubic shape of the dry NaCl particles and the water content of the $NaNO_3$ droplets in the first DMA are considered in the experimental growth factors.

Table A1. Coefficients for the calculation of the density of salt solutions (*18*).

Salt	$(NH_4)_2SO_4$	NaCl	$NaNO_3$
mass percent range	0-78	0-45	0-98
A_1	5.92	7.41	6.512
A_2	$-5.036 \cdot 10^{-3}$	$-3.741 \cdot 10^{-2}$	$3.025 \cdot 10^{-2}$
A_3	$1.024 \cdot 10^{-5}$	$2.252 \cdot 10^{-3}$	$1.437 \cdot 10^{-4}$
A_4	---	$-2.06 \cdot 10^{-5}$	---

Table A2. Coefficients for the calculation of the solution surface tension (*20*).

Salt	$(NH_4)_2SO_4$	NaCl	$NaNO_3$
β_s $[10^{-3}Nm^{-1}M^{-1}]$	2.17	1.64	1.12

Table A3. Coefficients to calculate the water activity of $(NH_4)_2SO_4$ solution.

Temperature	20 °C	-10 °C
ρ	13.0	13.0
α_{MX}	13.0	13.0
α^1_{MX}	1.50	1.50
A_x	2.8923	2.7634
B_{MX}	13.7298984	1.1043888
B^1_{MX}	-21.3757307	-47.3542891
$W_{w,MX}$	-2.29903871	-4.6021552
$U_{w,MX}$	2.165604209	2.564384665
$V_{w,MX}$	-2.1048037	-1.08506335

Table A4. Coefficients for the calculation of the osmotic coefficient of NaCl solution (*24*).

w_6	25.000115	w_{14}	119.32133
w_7	-653.05872	w_{15}	0.0014068
w_8	-4.4871462	w_{16}	-4.234548
w_9	0.010995543	w_{17}	0.40642361
w_{10}	-0.0000047	w_{18}	-6.1068702
w_{11}	-1.1938067	w_{19}	-0.07538385
w_{12}	5.4518092	w_{20}	0.000137088
w_{13}	-0.483091	w_{21}	0.27649564